First-principles Study of Defect Migration in RE-doped Ceria (RE = Pr, Gd)

Pratik Dholabhai[1], James Adams[1], Peter Crozier[1], and Renu Sharma[1,2]
[1]Materials Science & Engineering, Arizona State University, Tempe, AZ 85287
[2]Center for Nanoscale Science and Technology, National Institute of Standards and Technology, Gaithersburg, MD 20899

ABSTRACT

Oxygen vacancy formation and migration in ceria is central to its performance as an ionic conductor. Ceria doped with suitable aliovalent dopants has enhanced oxygen ion conductivity – higher than that of yttria stabilized zirconia (YSZ), the most widely used electrolyte material in solid oxide fuel cells (SOFC). To gain insight into atomic defect migration in this class of promising electrolyte materials, we have performed total energy calculations within the framework of density functional theory (DFT+*U*) to study oxygen vacancy migration in ceria, Pr-doped ceria (PDC) and Gd-doped ceria (GDC). We report activation energies for various oxygen vacancy migration pathways in PDC and GDC. Results pertaining to the preferred oxygen vacancy formation sites and migration pathways in these materials will be discussed in detail. Overall, the presence of Pr and Gd ions significantly affects oxygen vacancy formation and migration, in a complex manner requiring the investigation of many different migration events. We propose a relationship that explains the role of additional dopants in lowering the activation energy for vacancy migration in PDC and GDC.

INTRODUCTION

One of the most important components for intermediate temperature (500 °C to 750 °C) SOFCs is the electrolyte material, which should have very high oxide-ion conductivity in the intermediate temperature range. Oxygen-ion conductivity of doped ceria is reportedly higher than the most widely used solid electrolyte material, YSZ, at temperatures below 600 °C [1]. The various applications of PDC include but are not limited to its use as an oxide electrode having high electronic and ionic conductivity [2], cathode materials for SOFC [3], and for membranes for oxygen separation, where equally high electronic and ionic conductivities are required to achieve the maximum of oxygen flux through the membrane [4]. In comparison of traditional electrolyte materials, GDC is reported to be one of the most promising solid electrolyte materials for operation of SOFC below 600 °C [5,6]. Knowledge of the factors controlling oxygen vacancy diffusion in PDC and GDC is therefore valuable. Lower activation energies lead to higher oxide ion conductivity (Eq. (1)).

$$\sigma = \sigma_0 \exp(-E_a / k_B T) \qquad (1)$$

where σ is the ionic conductivity, E_a is the activation energy for oxygen vacancy diffusion, σ_0 is the pre-exponential factor, T is the absolute temperature and k_B is the Boltzmann constant. However, the activation energies for vacancy migration in these materials depend on the dopant concentration.

Calculations of the oxygen vacancy migration and formation in ceria-based materials have been performed previously, but there is only one study investigating vacancy migration in

PDC and GDC [7]. There, the authors investigated diffusion of oxygen vacancy adjacent to two dopants, and only a few jump events were studied. In order to develop a full model of diffusion, and to understand the effect of dopants in ceria, further calculations are needed. In this proceeding, we present a first principles based DFT+*U* study of different diffusion pathways for oxygen vacancy migration in PDC and GDC via a vacancy hopping mechanism. Any trivalent dopant in ceria-based materials has a complex effect on vacancy formation and migration. Our goal is to investigate all nearest neighbor and second nearest neighbor jump events among first, second, and third nearest neighbor sites which will contribute towards diffusion of vacancies in PDC and GDC. The calculation of the rate of each of these events will let us develop a Kinetic Lattice Monte Carlo (KLMC) model of vacancy diffusion in undoped and doped ceria that will allow the rigorous determination of the oxygen ion.

COMPUTATIONAL DETAILS

For all cases considered, spin-polarized calculations have been performed within the generalized gradient approximation to density functional theory (GGA-DFT)[8] with the Perdew-Burke-Ernzerhof exchange-correlation functional [9]. We have applied the rotationally invariant form of GGA+*U*, a combination of the standard GGA and a Hubbard Hamiltonian for the Coulomb repulsion and exchange interaction, formulated by Dudarev et al. [10] to account for the strong on-site Coulomb repulsion amid the localized Ce-4*f* electrons. The rationale for this approach is explained in references11 and 12. For the current calculations, a value of 5 eV has been chosen for the effective Coulomb parameter (U_{eff}). This choice of the empirical parameter U_{eff} = 5 eV for ceria and doped ceria is discussed in detail in reference 11.

Within the GGA+U formalism, the Kohn-Sham equations were solved using the plane wave basis and used with a projected augmented wave (PAW) [13,14], method as implemented in the Vienna Ab Initio Simulation Package (VASP) [15,16]. To assure accurate results, we used a plane-wave cut-off energy of 400 eV, which resulted in the convergence of the energies to approximately 0.01 meV. The irreducible Brillouin-zone integrations were performed using a Monkhorst-Pack grid of 2 × 2 × 2.

To simulate various systems, we have used a 96-atom (32 Ce and 64 O atoms, i.e. 8 elementary unit cells of CeO_2) supercell with a 2 × 2 × 2 periodicity built from a conventional 12-atom cubic unit cell of ceria. The supercell was built using the theoretically optimized lattice constant of 0.5494 nm for bulk ceria [11]. The PDC and GDC supercells were simulated by substituting two Ce ions with two trivalent Pr/Gd ions. The corresponding mole fraction of dopant is ≈ 6 %. Removing an oxygen ion to create an oxygen vacancy simulated reduced ceria and reduced PDC/GDC. The corresponding mole fraction of vacancy is ≈ 1.5 %. The doped systems were optimized with respect to cell parameter as well as atomic positions. For the reduced systems, the cell parameter was fixed at the corresponding unreduced value.

The activation energies for oxygen vacancy migration were determined by the difference between the total energy of the system before the migration of an oxygen ion and the saddle-point energy. The saddle-point positions were chosen as the midpoints along the line joining the initial and the final site for the migrating ion. To ensure that the midpoint is in fact the true maximum energy point, test calculations were performed for cases where the migrating ion was shifted slightly from the mid-point. These calculations showed that the mid-point is in fact the highest energy position. For all cases, the migrating ion was allowed to relax in the plane perpendicular to the migration path.

DISCUSSION

Oxygen vacancy formation in PDC/GDC and structural relaxations

In our models of PDC and GDC, there are different possible positions for creating an oxygen vacancy. We have only analyzed the cases where the oxygen vacancy is located at a first nearest neighbor (1NN), second nearest neighbor (2NN) and third nearest neighbor (3NN) with respect to the dopant ion. The second dopant ion is placed far apart from the respective Pr/Gd ion that is closer to the oxygen vacancy. This arrangement will enable us to understand the effect of a single dopant ion towards the activation energy for vacancy migration. Later we will address the case where two dopant ions are placed next to each other. In this context, we have studied nine different migration paths for an oxygen vacancy located at 1NN, 2NN or 3NN in PDC and GDC (see Figure 1). These paths are (1NN → 1NN), (1NN → 2NN), (1NN → 3NN), (2NN → 1NN), (2NN → 2NN), (2NN → 3NN), (3NN → 1NN), (3NN → 2NN) and (3NN → 3NN). We have only evaluated activation energies for NN and next-NN migration paths, since they are expected to have the lowest energy barriers.

We calculated oxygen vacancy formation energies at different positions with respect to a dopant ion in PDC and GDC. The formation of an oxygen vacancy at 2NN position in PDC is found to be the most favorable. This is contrary to the results obtained for GDC, where the 1NN position was found to be the most favorable for vacancy formation. The ionic radius of Gd^{3+} ion (0.1193 nm) is closer to the ionic radius of the host Ce^{4+} ion (0.1110 nm) as compared to that of Pr^{3+} ion (0.1266 nm). The volume readily available in GDC for an oxygen vacancy formation is larger at 1NN than that in PDC. Our results are in agreement with Andersson *et al*. [7] who reported that the formation of an anionic vacancy is correlated to the ionic radius of the dopant ion, with 1NN position favorable for dopant ions with ionic radius closer to the host cation, and 2NN position favorable for dopant ions with ionic radius considerably larger than the host cation.

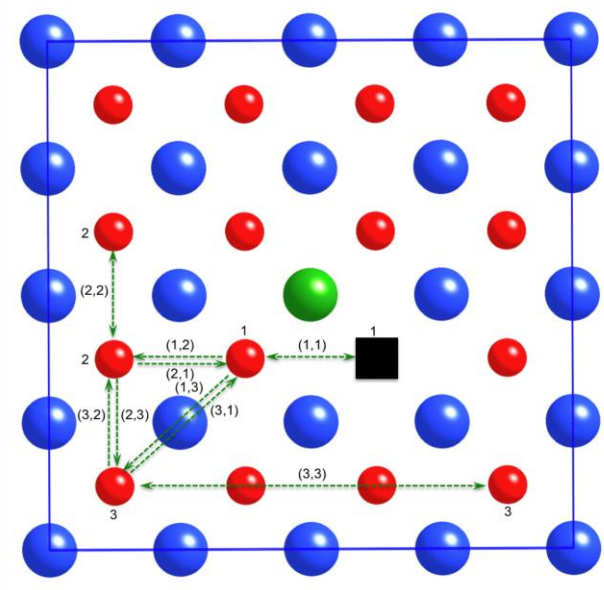

Figure 1. Top view of a 2 x 2 x 2 doped supercell. The larger balls represent Ce/Pr/Gd ions and the smaller balls represent oxygen ions, respectively. Numbers 1, 2 and 3 represent 1NN, 2NN and 3NN oxygen ions with respect to the dopant ion, respectively. Black box represents the oxygen vacancy. (X, Y) represents an oxygen ion jump from X NN to Y NN and the arrows

show the direction of jump. The dopant ion closer to the migrating vacancy is only shown, which is in the centre of the supercell.

This is also consistent with our results for PDC [11] and GDC [12]. The 3NN position for an oxygen vacancy formation is found to be least favorable in both PDC and GDC, as the dopant-defect interaction diminishes at this distance, which is large enough for them to be considered isolated. This scenario can be considered analogous to the formation of an oxygen vacancy in bulk ceria. For all three cases (oxygen vacancy in the 1NN, 2NN and 3NN positions) for PDC and GDC, the relaxation of the oxygen ions results in decreasing Ce – O distances and increasing O – O distances around the oxygen vacancy. The observed structural relaxation is primarily due to electrostatic effects; cations move away from the vacancy as the ionized oxygen vacancy corresponds to a net effective positive charge, and anions move towards the vacancy.

Oxygen vacancy migration in PDC/GDC and comparison with experiment

Listed in Table 1 are the activation energies for the nine different pathways for oxygen vacancy migration in PDC and GDC. The activation energies for vacancy migration in PDC and GDC along the path 1NN → 1NN are 0.78 eV and 0.59 eV respectively. These energies are higher than those for the respective 2NN → 2NN and 3NN → 3NN paths. This effect can be attributed to the presence of larger Pr^{3+}/Gd^{3+} ion along the 1NN → 1NN path that leaves less conduction space for an oxygen ion to move through the saddle point.

For the 2NN → 2NN and 3NN → 3NN jumps, the local environment is different in that the initial and final position of the migrating oxygen ion is surrounded by smaller Ce^{4+} ions. Hence these migration paths are analogous to the case where the oxygen ion is migrating in bulk ceria as they are directed far away from the dopant and hence show energetics similar to those for migration in bulk ceria. The activation energies for vacancy migration along the paths 1NN → 2NN and 2NN → 1NN in GDC are 0.50 eV and 0.36 eV respectively. For the same paths, the

Table 1. Calculated activation energies (E_a) for oxygen vacancy migration in ceria and for different pathways in PDC and GDC (uncertainty in energies is ≈ 0.01 meV). E_{Bulk} is the activation energy for bulk diffusion in ceria, whereas $E_{(X,Y)}$ denotes activation energy for a oxygen atom migrating from XNN to YNN in PDC and GDC.

Migration pathway	PDC [11] E_a (eV)	GDC [12] E_a (eV)	Migration pathway	PDC [11] E_a (eV)	GDC [12] E_a (eV)
E_{Bulk}	0.47		$E_{(2,2)}$	0.47	0.48
$E_{(1,1)}$	0.78	0.59	$E_{(2,3)}$	0.57	0.49
$E_{(1,2)}$	0.41	0.50	$E_{(3,1)}$	2.69	2.46
$E_{(1,3)}$	2.79	2.61	$E_{(3,2)}$	0.44	0.46
$E_{(2,1)}$	0.43	0.36	$E_{(3,3)}$	0.47	0.47

values for PDC are 0.41 eV and 0.43 eV. It is found that the movement of an oxygen ion from a less favorable to a more favorable vacancy formation site (2NN →1NN) is preferred. The activation energy for the most favorable migration path 2NN → 1NN in GDC is lower by 0.11 eV as compared to the bulk migration energy, whereas in PDC, the most favorable path 1NN →

2NN is lower by 0.06 eV as compared to bulk migration. This suggest that for specific migration paths, GDC works better and for some PDC works better, but for evaluating the overall performance of the material, additional jump events or a KLMC model is essential. The activation energies for vacancy migration along the paths 1NN → 3NN and 3NN → 1NN for both the materials is the least favorable. These jump events will be very rare, and will contribute little to diffusion.

The various activation energies in doped ceria reported above can be attributed to the geometric relaxations of the cations and anions in the vicinity of the larger trivalent dopant ion and the larger volume available in doped ceria for the formation of an oxygen vacancy. A number of different diffusion pathways exist in an oxide ion conductor. Determination of the rate-limiting step for a path is complex, because it depends on the dopant concentration and arrangement. For example, in the case of GDC, the activation energy for the jump 2NN → 1NN is the lowest (0.36 eV), but that is not a complete path – a vacancy cannot diffuse a long distance along that path. A vacancy has to subsequently jump from 1NN → 2NN to diffuse a long distance. Hence, at high dopant concentrations, one possible path is 2NN → 1NN, followed by 1NN → 2NN, where the final 1NN site is different from the first (it may or may not be to the same dopant). Repeated jumps of this type form a continuous long-distance path, and the rate-limiting step for the path is the 1NN → 2NN (0.50 eV). At lower dopant concentrations, this path is unlikely to allow a vacancy to jump from one dopant to another; instead, additional jumps such as 1NN → 1NN, 2NN → 2NN, 2NN → 3NN, 3NN → 3NN or 3NN → 2NN may be required. The exact dopant concentrations and temperature at which different jumps would contribute towards the diffusion mechanism would require either a KLMC model or a complex percolation theory calculation.

To understand the change in activation energy for vacancy migration in the presence of multiple dopants, we calculated the activation energy of migration along the two migration paths 1NN → 2NN and 2NN → 1NN in the presence of two dopant ions placed next to each other. For these two migration paths we found that the decrease in activation energy for ceria doped with two dopant ions located next to each other was twice as much compared to ceria doped with two dopant ions that are separated. These results are in agreement with work done by Andersson *et al*. [7] Thus, it can be proposed that, at low dopant concentrations, the effect of additional dopants on activation energies is additive.

The calculated values for activation energies in this article should be considered as a first approximation in depicting the preferred migration pathway for vacancy diffusion, which improves the understanding of oxide ion conductivity in doped ceria. A direct comparison between our calculations and the experimental data requires the development of a diffusion model that incorporates the results of the present paper. In other words, these activation energies can be used as inputs to a KLMC model for simulating the vacancy diffusion in PDC and GDC. The activation energy values for a complete path via which a vacancy can diffuse should be weighed against the experimental data. The activation energies for some of the jump events in PDC and GDC are lower than or equal to the bulk activation energy in ceria, but the activation energy value for a complete diffusion path is slightly different.

CONCLUSIONS

PDC and GDC have been studied in detail by first-principles calculations to elucidate the oxygen vacancy migration in these systems, which occur via a vacancy hopping mechanism.

Activation energies for oxygen vacancy migration in PDC and GDC were evaluated by calculating the energy of the migrating oxygen ion in the saddle point position. For doped configurations, the oxygen vacancies were created at three different positions; 1NN, 2NN and 3NN with respect to the dopant ion to study the nine different migration paths. The formation of oxygen vacancy at 1NN and 2NN is found to be the most favorable for GDC and PDC respectively, owing to the larger volume available in this vicinity. The most favorable oxygen vacancy migration path in PDC was found to be 1NN → 2NN and that for GDC was 2NN → 1NN and the activation energy value for a complete migration path was found to be in reasonable agreement with available experimental results. We propose that every additional dopant ion in the vicinity of the migrating vacancy will have an additive effect towards decreasing the activation energy for migration, at low concentrations. The activation energies for oxygen vacancy migration along distinct pathways will be incorporated in a KLMC model for vacancy diffusion in doped ceria. The KLMC model will allow the rigorous determination of the oxygen ion conductivity as a function of temperature and dopant concentration and the results will be discussed in near future.

ACKNOWLEDGEMENTS

This work is supported by the Department of Energy under the Grant No. DE-PS02-06ER06-17. The authors gratefully acknowledge the Fulton High Performance Computing Initiative (HPCI) at the Arizona State University for the computational resources. P.P.D wishes to thank Shahriar Anwar for stimulating discussions.

REFERENCES

[1] M. Mogensen, N. M. Sammes, G. A. Tompsett, Solid State Ionics **129**, 63 (2000).
[2] Y. Takasu, T. Sugino, Y. Matsuda, J. App. Electrochem. **14**, 79 (1984).
[3] M. Nauer, Ch. Fticos, B.C.H. Steele, J. Eur. Ceram. Soc. **14**, 493 (1994).
[4] P. Shuk, M. Greenblatt, Solid State Ionics **116**, 217 (1999).
[5] B. C. H. Steele, A. Heinzel, Nature **414**, 345 (2001).
[6] B. C. H. Steele, Solid State Ionics **129**, 95 (2000).
[7] D. A. Andersson, S. I. Simak, N. V. Skorodumova, I. A. Abrikosov, B. Johansson, Proc. Natl. Acad. Sci. **103**, 3518 (2006).
[8] P. Hohenberg, W. Kohn, Phys. Rev., 1994 136, B864; W. Kohn, L. J. Sham, Phys. Rev. **140**, A1133 (1965).
[9] J. P. Perdew, K. Burke, M. Ernzerhof, Phys. Rev. Lett. **77**, 3865 (1996).
[10] S. L. Dudarev, G. A. Botton, S. Y. Savrasov, C. J. Humphreys, A. P. Sutton, Phys. Rev. B **57**, 1505 (1998).
[11] P. P. Dholabhai, J. B. Adams, P. Crozier and R. Sharma, J. Chem. Phys. **132**, 094104 (2010).
[12] P. P. Dholabhai, J. B. Adams, P. Crozier and R. Sharma, Phys. Chem. Chem. Phys. **12**, 7904 (2010).
[13] P. E. Bhochl, Phys. Rev. B **50**, 17953 (1994).
[14] G. Kresse, D. Joubert, Phys. Rev. B **59**, 1758 (1999).
[15] G. Kresse, J. Hafner, Phys. Rev. B **47**, 558 (1993).
[16] G. Kresse, J. Furthmuller, Phys. Rev. B **54**, 11169 (1996).